Observation of a first-order metal-to-nonmetal phase transition in fluid iron

V. N. Korobenko and A. D. Rakhel*

Joint Institute for High Temperatures of Russian Academy of Sciences, Izhorskaya 13, Bld. 2, 125412 Moscow, Russia

(Received 29 December 2011; published 30 January 2012)

Measurements of electrical resistivity and caloric equation of state have been performed for fluid iron to investigate the metal-to-nonmetal transition induced by thermal expansion. The resistivity results published earlier [V. N. Korobenko and A. D. Rakhel, JETP, **112**, 649 (2011)] have revealed the transition occurring at a density 4–5 times lower than ambient solid since in this density range the isochoric temperature coefficient of resistivity becomes negative when the magnitude of resistivity exceeds the minimum metallic conductivity range. The equation of state results reported here provide strong evidence for the existence of a first-order phase transition with a critical point located near the metal-to-nonmetal transition threshold. In particular, the isentropes plotted in the pressure-specific volume plane demonstrate pronounced kinks located on a convex line with a maximum at about 5 GPa. This suggests the presence of a critical point with the pressure of about one order of magnitude higher than that expected for the liquid-vapor transition. Arguments are given that the phase diagram of iron has the structure predicted in the well-known work [Ya. B. Zel'dovich and L. D. Landau, Zh. Eksp. Teor. Fiz. **14**, 32 (1944)] but has not been observed yet.

DOI: 10.1103/PhysRevB.85.014208 PACS number(s): 64.70.F−, 52.27.Gr, 71.22.+i, 71.30.+h

I. INTRODUCTION

A transition from metallic to a nonmetallic behavior can be observed in fluid metals thermally expanded to low density (at constant pressure).[1,2] One of the motivations of those experiments was to find out the structure of the phase diagrams of fluid metals in the liquid-vapor phase transition region since there had been predictions[3,4] that the metal-to-nonmetal (MNM) transition induced by thermal expansion can occur as an independent first-order phase transition with its own coexistence curve and the critical point. If so, the phase diagram, let's say in the pressure-temperature plane, contains two critical points and an additional triple point where three fluid phases are in equilibrium (rather than two as in the usual case).[3] To the best of our knowledge, to date, such first-order MNM transition, which is frequently called the discontinuous Mott transition, has not been detected.

The general belief in the existence of the first-order MNM transition is based on the idea that due to the long range Coulomb interaction there always exists a finite-size gap in the electron energy spectrum of an insulator[3,5] so that a continuous transition between the nonmetallic and metallic state is possible only at temperatures of the order of the gap width. The interplay between the Coulomb interaction and disorder has been a long-standing problem that is still far from understood.[6] From another point of view[7] the MNM transitions driven by the valence electrons density and disorder are continuous (in contrast to a first-order transition which becomes continuous at supercritical pressures). Since both points of view have not been proved rigorously so far the question about the influence of the MNM transition on thermodynamic functions and, in particular, about the interrelation between the MNM and the liquid-vapor phase transition remains open. At present this problem can hardly be solved theoretically since we do not have a theory that is able to predict the critical point parameters of the liquid-vapor phase transition. On the other hand, the approach developed in Ref. 7 cannot be applied to fluid metals since in the limit $T \to 0$ (at constant density) there is the liquid-vapor phase transition not included in the theoretical concept. Hence, to cast a light on the problem the experimental studies on the fluid metals with different atomic structure in wide ranges of density and temperature are needed.

The whole range of the liquid-vapor phase transition (including the critical point) has been investigated experimentally for mercury and the two alkali metals, **Cs** and **Rb**.[1,2] The experiments did not reveal any jumps in thermodynamic functions except those found in the liquid-vapor phase transition region. It should be noted that recently the small angle x-ray scattering experiments[8] have provided some evidence for the existence of an independent first-order MNM transition in liquid mercury. Nevertheless the situation remains unclear since no reliable indications of the transition have been found in thermodynamic functions.

The MNM transition observed in mercury (and in the alkali metals) occurs in the liquid state so that near the liquid-vapor critical point both the liquid and the gaseous phase are nonmetals. This can be seen by comparison of the value of electrical conductivity near the critical point (σ_c) with the minimum conductivity measured in the metallic state ($\sigma_{\min}$). Indeed, the main difference of a nonmetal from metal is the energy gap (or a mobility gap[4]) in the electron energy spectrum. The presence of the energy gap can be probed by the measurements of the electrical conductivity, which in a nonmetallic state acquires the activated dependence[4]

$$\sigma = \sigma_{\min} \exp[-\Delta/kT], \tag{1}$$

where Δ is proportional to the gap width in the electron density of states, T is temperature, and k is the Boltzmann constant. The pre-exponential factor $\sigma_{\min}$ characterizes the conductivity in the metallic state where the temperature dependence saturates (the Ioffe-Regel limit).[6,9] The typical values of the minimum inactivated conductivity for the majority of metals is $\sigma_{\min} = (3\text{–}5)\ 10^5\ \Omega^{-1}\ \mathrm{m}^{-1}$, but for some strongly correlated systems (such as the high-T_c cuprates) it can be 1.5–2 times less. As follows from the measurements[1,2,10] for mercury $\sigma_c \sim 10^2\ \Omega^{-1}\ \mathrm{m}^{-1}$ and for the two alkali metals $\sigma_c = 2\text{–}3\ 10^4\ \Omega^{-1}\ \mathrm{m}^{-1}$, and therefore the following inequality holds: $\sigma_c \ll \sigma_{\min}$.

This suggests that the critical points are of the same kind as in the insulating substances rather than due to the discontinuous Mott transition for which we expect $\sigma_c \sim \sigma_{\min}$. Such conclusion is consistent with estimates of the critical compressibility ratio $Z_c = AP_cV_c/RT_c$, where A is atomic weight; R is universal gas constant; and P_c, T_c, V_c are the critical pressure, temperature, and specific volume, respectively. A similarity between the critical points of different substances manifests itself in close values of the dimensionless parameter Z_c.[11] Since the value for mercury ($Z_c \approx 0.37$) and for the alkali metals ($Z_c = 0.22$–0.26) is rather close to those of the noble gases ($Z_c \approx 0.3$) and the van der Waals gas ($Z_c = 3/8$), the critical points of the three fluid metals are most likely similar to those of the noble gases rather than that of the first-order MNM transition. In the last case the critical pressure is expected to be essentially higher than the liquid-vapor critical point.[3]

The atomic structure of iron differs essentially from that of mercury and the alkali metals. The strong sp-d hybridization of the atomic orbitals, appearance of magnetism, and the spin-orbital interaction can affect essentially the MNM transition.[6,12] In the present study we demonstrate that in fluid iron the transition occurs as a first-order phase transition up to a critical point with an unexpectedly high critical pressure (about 5 GPa). We show that the equilibrium line of the phase transition in the density-pressure plane differs essentially from that of the liquid-vapor phase transition, and the phase diagram of fluid iron probably has the structure predicted in Ref. 3, i.e., it contains two critical points and an additional triple point.

Our approach is based on the simultaneous measurements of electrical resistivity and the caloric equation of state of fluid iron in wide ranges of density and pressure. The measurements of resistivity allow us to identify the occurrence of the MNM transition while the equation of state results to reveal a first-order phase transition.

II. EXPERIMENT

Specific internal energy E and resistivity σ^{-1} have been measured as functions of pressure P and specific volume V using the newly developed experimental technique.[13] This technique allows the measurements to be performed at temperatures of 1–3 eV and pressures of 1–10 GPa with an uncertainty less than 10%. The essence of the experimental technique is as follows. A piece of an iron foil strip is sandwiched between two flat sapphire plates and heated by an electrical current pulse with a density of (1–3) 10^7 A/cm^2. The heating conditions are chosen so that the spatial distributions of pressure and temperature in the foil sample experiencing a 5–10-fold thermal expansion for $t \sim 1$ μs remain sufficiently uniform.[13,14] This experimental technique had been succesfully utilized in the measurements of resistivity and caloric equation of state of fluid aluminum and provided the fairly accurate results.[13,14] A schematic of the experiments, as well as the diagnostics utilized, is shown in Fig. 1.

In the present experiments the foil strips of pure iron (99.9% Fe) of 30-μm thickness, 3–6 mm width, and 10 mm length together with a ruby plate (with a thickness of 380 μm, a width of 10 mm, and length of 10 mm) were placed between optically polished sapphire plates of 1.5–5 mm thickness. The

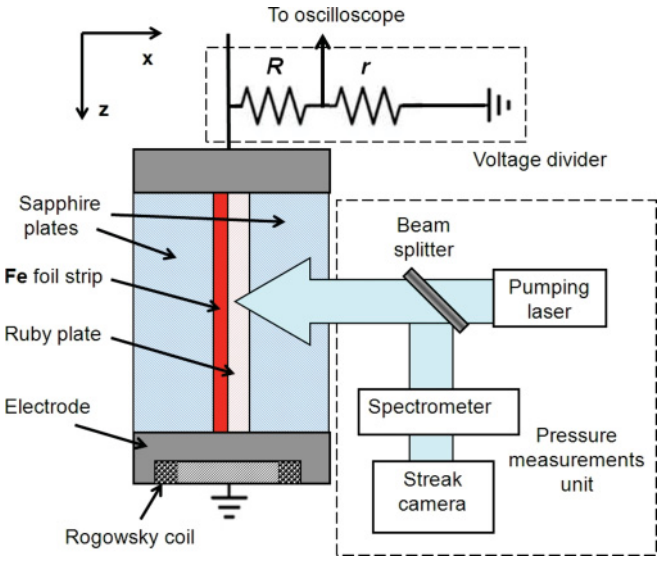

FIG. 1. (Color online) Schematic of the experiments. An iron foil strip placed together with a ruby plate between two sapphire plates is shown in the plane perpendicular to the surface of the strip. Electrical current flows along the z axis, and the sample undergoes thermal expansion predominantly along the x axis since the sample thickness is much smaller than its width and length and because the foil strip is sandwiched between flat (optical quality) and thick sapphire plates.

ruby plate was used to measure pressure by recording the ruby luminescence lines shifts. The experimental assembly was carefully glued by an epoxy resin so that the thickness of the apoxy layer between the sample and the ruby and sapphire plates did not exceed 3 μm. On the side of the ruby plate facing the sample, a multilayer dielectric mirror of about 2-μm thickness was deposited. This mirror reduced the thermal radiation that was an interference and increased the signal of the ruby luminescence. To heat the sample a capacitor bank discharge was used.[15] In each experiment we measured the temporal dependence of the current through the sample $I(t)$, the voltage drop along its length $U(t)$, and the pressure in the ruby plate near the sample $P(t)$. Resistance R and the specific Joule heat dissipated q were determined as follows:

$$R(t) = U_R(t)/I(t), \tag{2}$$

$$q(t) = M^{-1}\int_0^t I(t')U_R(t')dt', \tag{3}$$

where $U_R(t) = U(t) - L_f dI(t)/dt$ is the active voltage drop, M is the sample mass, and L_f is its inductance. From the measured temporal dependence of pressure $P(t)$ the sample volume was determined by solving the inverse problem about the motion of flat piston in a medium whose equation of state is known and the pressure on the piston is a given function of time.[13] The equation of state of sapphire within the range of uniaxial elastic deformation ($P < 12.5$ GPa) is known with an uncertainty $<1\%$. As the difference between the mechanical properties of sapphire and ruby can be neglected (due to the low concentration of chromium in the ruby plates), the integration of the equations of motion can be performed with almost the same accuracy. After the sample volume is determined the mechanical work performed by it on the sapphire plates can

be calculated. The specific internal energy E is the difference between the specific Joule heat q and the work (per unit mass). Resistivity was calculated by the formula:

$$\sigma^{-1} = R(t)D(t)H/L,$$

where $D(t)$ is the sample thickness, and H and L are its width and length (assumed to be constant).

In these experiments we have measured a family of dependences of resistivity σ^{-1} and specific internal energy E on pressure P and specific volume V along the thermodynamic paths representing our experiments in the (P, V) plane. By varying the heating conditions and increasing the number of the experiments the region of interest in the (P, V) plane has been filled by the thermodynamic paths with a sufficient density to build isochores in the (E, P) plane or isobares in the (E, V) plane. Other details of the experimental technique can be found elsewhere.[13,15,16]

III. RESULTS

In Fig. 2 we show the dependence of resistivity on specific internal energy along several isochores to demonstrate the occurrence of the MNM transition in fluid iron. The isochores are labeled by the values of the relative volume $\varphi = V/V_0$, where the specific volume of solid iron at normal conditions $V_0 \approx 0.127$ cm^3/g. As seen, our measurements agree well with the data of Ref. 17. The usage for the analysis of the recently published results,[18] presented in further discussion, is made difficult by a 30–50% scatter; for this reason we do not show those data points. From Fig. 2 it follows that in the range of $\varphi = 2$–5 the slope of the isochores changes sign. This means that the isochoric temperature coefficient of resistivity $(\partial\sigma^{-1}/\partial T)_V$ also changes sign because

$$(\partial\sigma^{-1}/\partial E)_V = (\partial\sigma^{-1}/\partial T)_V/(\partial E/\partial T)_V,$$

and the specific heat $c_V = (\partial E/\partial T)_V > 0$. Such behavior of resistivity indicates a transition to a nonmetallic state in which conductivity takes the form (1). As seen in Fig. 2, the isochores become horizontal when resistivity attains 3–5 $\mu\Omega$ m, which is very close to the values of $(\sigma_{\min})^{-1}$ for the high-T_c cuprates.[9] Thus, the measurements' results indicate the occurrence of the MNM transition since the temperature coefficient of resistivity changes sign from positive to negative as soon as resistivity exceeds the minimum metallic conductivity range. Such behavior has been observed in many systems[6] and is usually regarded as a crossover between metallic and nonmetallic regimes of conductivity not affecting thermodynamic functions. In our experiments the MNM transition was observed at pressures $P = 2$–10 GPa, which are essentially higher than the critical pressure of the liquid-vapor phase transition, 0.8–1.0 GPa.[11,19,20] In this case one would expect that the MNM transition is continuous, but as we shall see the equation of state results indicate the contrary. It should be noted that the data presented in Fig. 2 have been partially published in Ref. 16. We present some of the isochores here again since they are indispensable for a consistent interpretation of the equation of state and resistivity results.

In Fig. 3 isochores have been plotted in the (P, E) plane. As seen, the figure strongly suggests that isochores $\varphi = 4$–6 have kinks at $P = 4$–5 GPa. For isochore $\varphi = 4$ we can locate

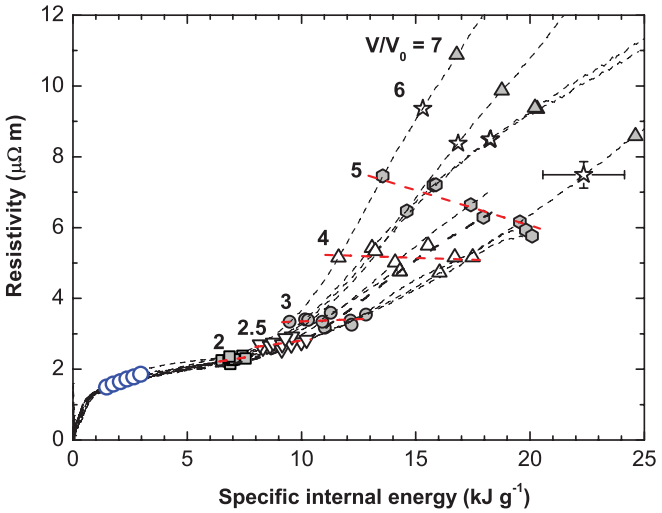

FIG. 2. (Color online) Resistivity of iron as a function of specific internal energy along isochores. The black dashed lines are dependencies measured in our experiments, and the blue open circles represent data.[17] The work values for seven isochores are shown with black (gray and open) marks; red dashed lines are linear fits of some of the isochores. The isochores change the slope from positive to negative when the minimum metallic conductivity range, 2–6 $\mu\Omega$ m, is exceeded.

the kink rather accurately, while for the other two isochores ($\varphi = 5$ and $\varphi = 6$), due to the small amount of the data points at $P > 5$ GPa, this cannot be done. Nevertheless, it is obvious that the data points on these isochores at $P > 5$ GPa cannot be approximated by the same fits determined at $P \leqslant 5$ GPa. It is well known that for a first-order phase transition the isochores must have kinks on the equilibrium line.[21] Thus, Fig. 3 provides an evidence for a first-order phase transition at $P \leqslant 5$ GPa. To locate the equilibrium line at $P < 4$ GPa

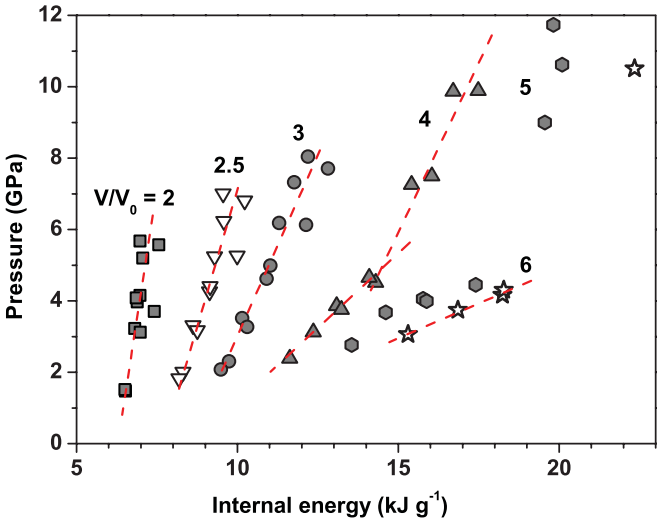

FIG. 3. (Color online) Pressure as a function of specific internal energy along isochores. The meaning of the symbols is the same as in Fig. 2. The red dashed lines show linear fits for isochores $\varphi = 2$–3 and for parts of isochores $\varphi = 4$–6. Fitting of isochores $\varphi = 4$–6 by piecewise linear functions reveals kinks in the pressure range of 4–5 GPa.

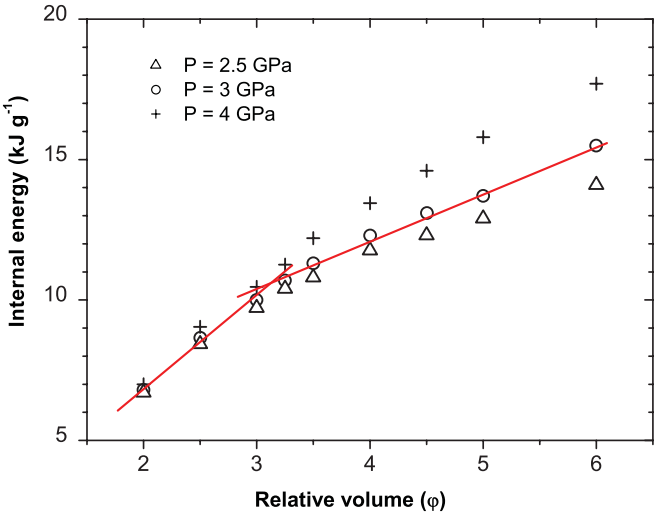

FIG. 4. (Color online) Internal energy as a function of relative volume along isobars. The data on isobar $P = 3$ GPa are fitted by piecewise linear function to locate the kink.

we have plotted isobars in the (E, V) plane. It can be easily shown that such isobars must have kinks on the equilibrium line as well and in the two-phase region they must be straight lines. This property of the isobars can be used to prove with a more degree of certainty the presence of the first-order phase transition. Indeed, in the two-phase region the specific internal energy and specific volume can be presented as follows:

$$E = E_1(P)(1 - x) + E_2(P)x \tag{4}$$

$$V = V_1(P)(1 - x) + V_2(P)x, \tag{5}$$

where the subscript denotes the phase, and x is the mass fraction of phase 2; it is assumed that in the two-phase state the system is near thermodynamic equilibrium. By differentiating Eqs. (4) and (5) with respect to volume at constant pressure we find the relation

$$\left(\frac{\partial E}{\partial V}\right)_P = \frac{E_2(P) - E_1(P)}{V_2(P) - V_1(P)}, \tag{6}$$

which proves the linearity of the isobars in the two-phase region. The isobars of fluid iron are shown in Fig. 4. As one can see, to within the uncertainty of the measurements in the two-phase region ($V/V_0 > 3$, $P < 5$ GPa), the isobars can be well fitted by straight lines and the locations of the kinks on the isobars reasonably agree with those determined from Fig. 3.

To validate the conclusion about the presence of the first-order phase transition we plotted also isentropes in the (P, V) plane. Kinks on isentropes are widely used for detecting the liquid-vapor phase transition which occurs during $t \sim 1$ μs in the rarefaction waves.[22,23] To build an isentrope we chose first an initial point (P_1, V_1) on the curve representing one of our experiments (let's say experiment **A**) and approximated the isentrope in a vicinity of the point by a linear function of volume $P = P_1 - a_1^2(V - V_1)$, where $a_1 = c_1/V_1$, and c_1 is sound speed. The dependence of internal energy on volume along the isentrope was found by integration of the relation $P = -(\partial E/\partial V)_S$. As a result we got the formula

$$E - E_1 = -\tfrac{1}{2}(P + P_1)(V - V_1), \tag{7}$$

where E_1 is a value of internal energy at the initial point.[24] To find the point at which the isentrope intersects the path representing another experiment (an experiment **B**) approaching sufficiently close to the initial point, we substituted the measured dependence $E_B(V)$ and $P_B(V)$ for experiment **B** in Eq. (7) and solved it for the value of specific volume.

As seen in Fig. 4, the isentropes indeed demonstrate pronounced kinks at the values of pressure and relative volume where the kinks on isochores and isobars have been found. The blue convex curve shows a smooth fit to the kinks positions. The curve has a maximum (or at least it saturates) at $P \approx 4.7$ GPa, which suggests a critical point with so high pressure. In Fig. 5 we presented as well several isentropes obtained using another approach.[25] The isentropes were found by integration of the equation

$$\left(\frac{\partial P}{\partial V}\right)_S = -\left[\left(\frac{\partial E}{\partial V}\right)_P + P\right] \Big/ \left(\frac{\partial E}{\partial P}\right)_V, \tag{8}$$

in which the partial derivatives of internal energy in respect to specific volume and pressure were determined in an analytical form. It turned out that in the region of the (P, V) plane where the partial derivatives $(\partial E/\partial P)_V$ and $(\partial E/\partial V)_P$ could be determined accurately, the isentropes practically coincide with those found from Eq. (7). The comparison demonstrates that the uncertainty in the values of pressure and volume on the isentropes found by the method proposed here (and which

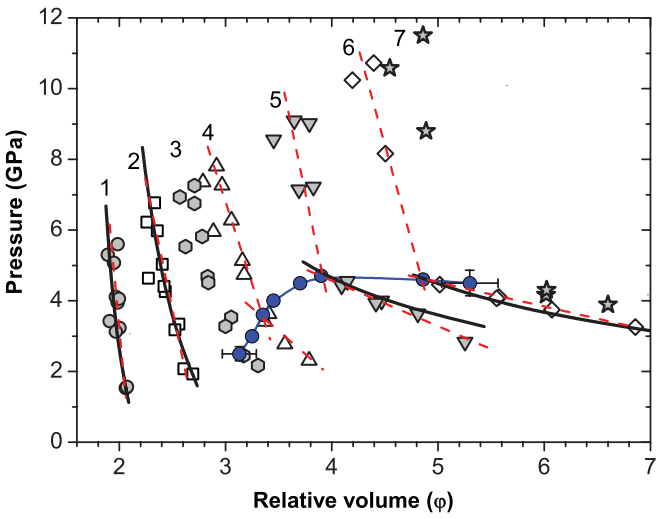

FIG. 5. (Color online) Pressure as a function of relative volume along isentropes. The black (gray and open) marks correspond to seven fixed entropy values obtained by Eq. (7). Four isentropes determined by integration of Eq. (8) are shown with the thick black lines (isentropes 1, 2, and portions of isentropes 5 and 6 at $P < 5$ GPa). The data on isentropes were approximated by piecewise linear functions (the red dashed lines) to locate the kinks. The blue circles are the kinks' positions determined for some of the isentropes, the isobars shown in Fig. 4, and the isochores in Fig. 3. The blue convex line connecting the points shows tentatively the equilibrium line of the first-order phase transition.

was used in the region where the partial derivatives are poorly defined) does not exceed the measurements uncertainty.

As can be seen from Fig. 5 for isentropes 4–6, the sound speed $c_s = V\sqrt{-(\partial P/\partial V)_S}$ undergoes a jump from about 3–4 km/s in the one-phase state down to 1.5–2.0 km/s in the two-phase region. The question concerning kinetics effects arises. Since the kinks on isentropes (and isobars) are clearly manifested so that the phase transition is fast, these effects play obviously a minor role. On the other hand, the relatively low values of sound speed in the two-phase region may increase the measurements uncertainty due to a non-uniform expansion of the sample. Our estimates show that for $P > 3$ GPa these uncertainties are insignificant.

IV. DISCUSSION

The interpretation of the resistivity results, assuming that the MNM transition is continuous, has been given in Ref. 16. Since actually it is not the case, the interpretation should be revised. As seen from Figs. 2–5, resistivity at isobar $P = 4$ GPa (which must be an isotherm in the two-phase region) increases from about 4 $\mu\Omega$ m in the metallic phase near the equilibrium line ($\varphi_1 \approx 3.4$) to 9–11 $\mu\Omega$ m in the nonmetallic phase (if at the equilibrium line $\varphi_2 = 6$–7). Thus, there is a remarkable discontinuous jump in resistivity. Let's assume the system in the two-phase state is a fine dispersed mixture of the metallic and nonmetallic phase whose conductivity can be described by the effective medium formula.[26] The equilibrium line shown in Fig. 5 is rather flat so that at $P \leqslant 4$ GPa the metallic phase conductivity on the equilibrium line (σ_1) is much higher than that of the nonmetallic phase (σ_2). Neglecting the conductivity of the nonmetallic phase, the effective medium formula can be written as follows:

$$\sigma_{\text{eff}} \approx \sigma_1(T)\left(1 - \frac{3}{2}y_2\right), \tag{9}$$

where y_2 is the volume fraction of the nonmetallic phase ($y_2 < 2/3$). Thus, the constant values of resistivity on isochores $\varphi = 3$–4 in Fig. 2 can be explained by the fact that the increase of resistivity with temperature in the metallic phase is compensated by a decrease in the volume fraction y_2, which turns to zero at the equilibrium line (if the critical volume $\varphi_c = 4$–5). The remarkably higher values of resistivity on isochores $\varphi = 5$–7 are due to the nonmetallic states with remarkably larger values of φ than the average ones (since the equilibrium line is flat).

The effective medium formula (9) predicts a percolation threshold at $y_2 = 2/3$. Density of the two-phase mixture at the percolation threshold is

$$\rho_p = (\rho_1(T) + 2\rho_2(T))/3,$$

where ρ_1 and ρ_2 are densities of the metallic and nonmetallic phase on the equilibrium line correspondingly. At low temperatures where $\rho_1 \gg \rho_2$, $\rho_p \approx \rho_1/3$ and it approaches the critical density at the critical temperature. Thus, in our experiments for which pressure did not vary essentially when the sample was in the two-phase state so that the process was approximately isothermal, the resistivity results must indicate the percolation threshold by an abrupt change in resistivity at about the critical density. As seen in Fig. 6 for the experiments satisfying this condition, the derivative $d\sigma^{-1}/d\varphi$ indeed has a maximum near the value $\varphi \approx 4$.

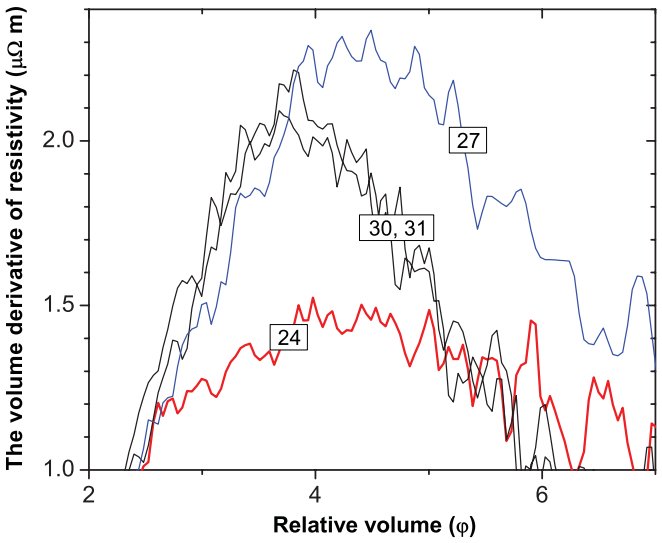

FIG. 6. (Color online) The volume derivative of resistivity $d\sigma^{-1}/d\varphi$ vs relative volume for three experiments (27, 30, and 31) whose thermodynamic paths crossed the two-phase region (and pressure was practically constant) and experiment 24, for which it was not the case. The maximum values of the derivative are located close to the critical volume $\varphi_c \approx 4$.

As follows from Figs. 2–4, near the critical point $\varphi = 4$–5, the resistivity in the one-phase state is within the range of 5–6 $\mu\Omega$ m that is very close to the minimum metallic conductivity range of the high-T_c cuprates.[6] Thus, the MNM transition in fluid iron occurs as a first-order phase transition up to the critical point. The first-order MNM transition can either coincide with the liquid-vapor phase transition or have its own equilibrium line.[3] To find out what is the case for iron, we have plotted the portion of the equilibrium of the here-observed

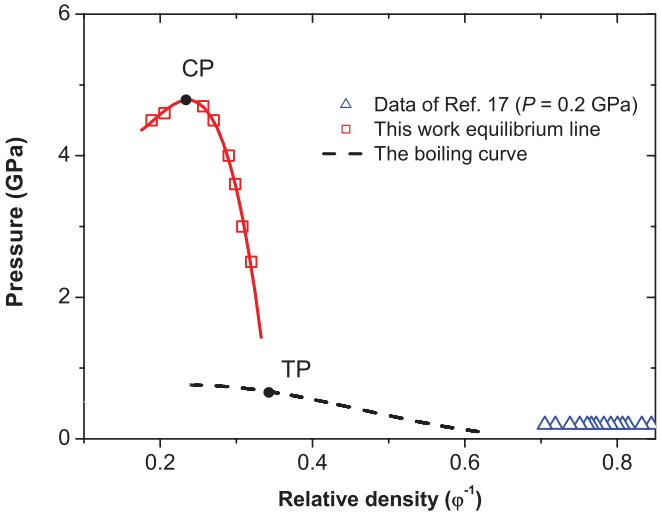

FIG. 7. (Color online) Portion of the equilibrium line of the phase transition determined in this work (red solid line) is compared with the boiling curve of iron (black dashed line) obtained by the soft-sphere equation of state.[27] CP is the MNM transition critical point; TP is the hypothetical triple point.

phase transition in the (P, φ^{-1}) plane and compared it with the boiling curve obtained by the soft-sphere equation of state,[27] whose parameters were fitted to the experimental values at low pressures.

As one can see in Fig. 7, the slope of the equilibrium line of the phase transition observed here is essentially steeper than that of the boiling curve. This strongly suggests that there is a triple point at which the boiling curve intersects the equilibrium line of the MNM transition at certain (nonzero) angle, i.e., there is a kink on the equilibrium line. Consequently, the phase diagram is of the form predicted in Ref. 3 (case no. 3) with an additional triple point and two critical points. The second critical point is located obviously at essentially lower pressure than that shown in Fig. 7 but above the triple point, $P_{TP} = 0.5$–0.8 GPa.

A noteworthy feature of the observed-here phase transition is the large values of internal energy on the equilibrium line which exceed essentially the sublimation energy of iron ($E_{\text{sub}} = 7.4$ kJ/g, Ref. 28). Nevertheless such behavior is not unique and has been observed in some fluids.[29] The unique nature of the present critical point becomes evident when we calculate the critical compressibility ratio Z_c. Estimating the critical temperature by means of the procedure[24] we get $Z_c \approx 2$, which is about one order of magnitude higher than the value for mercury, the alkali metals, and the noble gases.

Since on the nonmetallic side of the MNM transition, internal energy approaches the ionization energy of ions with the charge state $z = 1$–2, the thermodynamic states correspond to a dense plasma. However, the plasma-phase transition predicted for the gaseous state between two nonmetallic phases (see, e.g., Ref. 30 and the literature therein) seems to have no direct relation to the observed-here MNM transition. In our case the metallic phase is strongly degenerate and is hardly a gas. It seems that more relevant is the first-order MNM transition predicted for liquid hydrogen.[31] In that case metallization becomes continuous when pressure is above a critical point at which $\sigma_c \approx \sigma_{\min}$ and $Z_c \approx 8$.

V. CONCLUSION

In summary, we have detected a first-order phase transition in fluid iron with a critical point at about 5 GPa. This transition coincides with the MNM transition up to the critical point. Comparison of the equilibrium line of the phase transition with the boiling curve of iron suggests that the phase diagram has the structure predicted in Ref. 3.

ACKNOWLEDGMENTS

We express our gratitude to A. I. Savvatimskiy for management of the work on preparation of the sapphire and ruby plates and V. E. Fortov for constructive criticism. We should also like to thank I. L. Iosilevskiy, W. J. Nellis, and P. Noiret for useful suggestions and comments. This work was supported by the Basic Research Program of the Presidium of RAS P-09 "Study of matter under extreme conditions."

*rakhel@oivtran.ru

[1] G. Franz, W. Freyland, and F. Hensel, J. Phys. **41**, C8 (1980).
[2] I. K. Kikoin and A. P. Senchenkov, Fiz. Met. Metalloved. **24**, 843 (1967).
[3] Ya. B. Zel'dovich and L. D. Landau, Zh. Eksp. Teor. Fiz. **14**, 32 (1944).
[4] N. Mott, Rep. Prog. Phys. **47**, 909 (1984).
[5] R. E. Peierls, *Quantum Theory of Solids* (Oxford University Press, USA, 1996).
[6] V. F. Gantmakher, *Electrons and Disorder in Solids* (Nauka, Moscow, 2003; Oxford University Press, Oxford, 2005).
[7] E. Abrahams, P. W. Anderson, D. C. Licciardello, and T. V. Ramakrishnan, Phys. Rev. Lett. **42**, 673 (1979).
[8] M. Inui, K. Matsuda, D. Ishikawa, K. Tamura, and Y. Ohishi, Phys. Rev. Lett. **98**, 185504 (2007).
[9] O. Gunnarsson, M. Calandra, and J. E. Han, Rev. Mod. Phys. **75**, 1085 (2003).
[10] F. Hensel, Phil. Trans. R. Soc. Lond. A **356**, 97 (1998).
[11] V. E. Fortov, A. N. Dremin, and A. A. Leont'ev, High Temp. **13**, 1072 (1975).
[12] N. F. Mott and E. A. Devis, *Electron Processes in Non-Crystalline Materials* (Clarendon Press, Oxford, 1979).
[13] V. N. Korobenko and A. D. Rakhel, Phys. Rev. B **75**, 064208 (2007).
[14] J. Clérouin, P. Noiret, V. N. Korobenko, and A. D. Rakhel, Phys. Rev. B **78**, 224203 (2008).
[15] V. N. Korobenko, A. D. Rakhel, A. I. Savvatimski, and V. E. Fortov, Phys. Rev. B **71**, 014208 (2005).
[16] V. N. Korobenko and A. D. Rakhel, JETP, **112**, 649 (2011).
[17] R. S. Hixson, M. A. Winkler, and M. L. Hodgdon, Phys. Rev. B **42**. 6485 (1990).
[18] A. W. DeSilva and G. B. Vunni, Phys. Rev. E **83**, 037402 (2011).
[19] K. Hornung, J. Appl. Phys. **46**, 2548 (1975).
[20] D. A. Young and B. J. Alder, Phys. Rev. A **3**, 364 (1971).
[21] L. D. Landau and E. M. Lifshitz, *Fluid Mechanics* (Pergamon Press, Oxford, 1992).
[22] L. V. Altshuler, A. A. Bakanova, A. V. Bushman, I. P. Dudoladov, and V. N. Zubarev, Sov. Phys. JETP **46**, 980 (1977).
[23] G. E. Duvall and R. A. Graham, Rev. Mod. Phys. **49**, 523 (1977).
[24] V. N. Korobenko and A. D. Rakhel, e-print arXiv:1101.0487v2 (2011).
[25] Ya. B. Zel'dovich, Zh. Eksp. Teor. Fiz. **32**, 1577 (1957).
[26] R. Landauer, J. Appl. Phys. **23**, 779 (1952).
[27] D. A. Young, Lawrence Livermore Laboratory, Report No. UCRL-52352 (1977).
[28] *Physical Quantities: Handbook*, edited by I. S. Grigorev and E. Z. Meylikhov (Energoatomizdat, Moscow, 1991).
[29] N. R. Nannan, Advancements in nonclassical gas dynamics, Ph.D. dissertation, thesis (Delft University of Technology, Netherland, 2009).
[30] W. Ebeling and G. Norman, J. Stat. Phys. **110**, 861 (2003).
[31] M. A. Morales, C. Pierleoni, E. Schweglerd, and D. M. Ceperley, PNAS **107**, 12799 (2010).